An Analog VLSI Model of the Jamming Avoidance Response in Electric Fish

John E. LeMoncheck

Abstract—**We describe an analog VLSI model of the jamming avoidance response (JAR) in the electric fish *Eigenmannia*. The fish uses the JAR to change the frequency of its electric organ discharge (EOD) so that interfering signals do not impair its ability to detect and locate objects with its electric field. This system, although behaviorally simple, comprises many levels of processing and distributes the computation over a number of locally connected elements. The distributed nature of the computation makes analog VLSI technology a good substrate for implementing this model because mismatches in the electronic components are averaged out and are therefore not a problem. We examine the chip's behavior, and compare its data to biological data as a qualitative measure of correctness. By modeling the JAR, we hope to gain insight into how we can combine the biological techniques with analog VLSI methods into a more general signal processing system.**

I. Introduction

RECOVERING a signal from a noisy or disrupted channel is a problem found in both nature and engineering. Although we have many engineering solutions to this problem, it is valuable to study the adaptive biological solutions so we may gain insight into methods to improve the performance of our current systems. The jamming avoidance response (JAR) in electric fish is one such biological filtering system. These fish both emit and detect time-varying electric fields that can be used for object detection and communication. The JAR takes information about the sensory environment and tunes the frequency of the emitted waveform to enhance the fish's ability to locate objects.

One sensory problem that these fish face is that signals from another fish can cause interference, which reduces the effectiveness of either fish's electrosensory system. In species that emit a sinusoid-like electric field, a characteristic beat pattern results from the interference of the two waves. This interference creates periods of very low-amplitude electric field where the signals interact destructively. The fish's object location ability is impaired during these low-amplitude periods, and the fish has difficulty navigating. To resolve these problems, the weakly electric fish *Eigenmannia* shifts the frequency of its emitted wave away from the interfering frequency [1]. Thus, the fish must be sensitive to the sign of the frequency difference between the two interacting waveforms.

Many species of electric fishes have no direct awareness of their own signal, and hence no direct frequency reference. Despite this fact, the fishes can accurately code the sign of the difference frequency by combining locally derived estimates of the beat pattern from many different patches of receptors located along their bodies. Because the global difference frequency is computed from a number of elements weighted by their activity, the computation is robust and redundant. We have modeled this jamming avoidance response and have built an analog VLSI implementation of it. By studying the behavior of the model, we may gain insight into how we can apply these techniques to an artificial signal processing system. Many of the biological structures used in the JAR contribute to the electrolocation ability of the fish [2], [3]. Thus, we are building a foundation for future models of the detection and location of objects from multiple sensory locations. The large number of sensors and the redundancy of information in the data pathway make a VLSI implementation ideal because the algorithm is relatively insensitive to individual component variation. By experimenting with the model, we can observe which elements are essential for adequate jamming avoidance. We can then have a better understanding of not only the biological system, but also how one can implement a robust, synthetic filtering system.

In this paper, we will describe the algorithm used for determining the correct sign of the frequency difference between a source sine wave and an interfering sine wave, and the architecture of the chip which implements this algorithm. The individual components of the architecture are described, and data are shown from each circuit component. Actual data from the model operating as a whole are given, along with equivalent biological data, so that a qualitative comparison between the two can be made.

II. Background

If we compare a wave made up of two sinusoids of frequencies f_1 and f_2 to a reference sinusoid of frequency f_1, we see that the peaks of the mixed wave travel around the peaks of the reference (Fig. 1(b)–(g)). If we plot the amplitude of the beat pattern versus phase difference, we sweep out a closed loop centered about zero phase and the average value of the amplitude. The direction in which

Manuscript received October 2, 1990; revised February 13, 1992. This work was supported by a grant from the Office of Naval Research.

The author is with the California Institute of Technology, Pasadena, CA 91125.

IEEE Log Number 9107757.

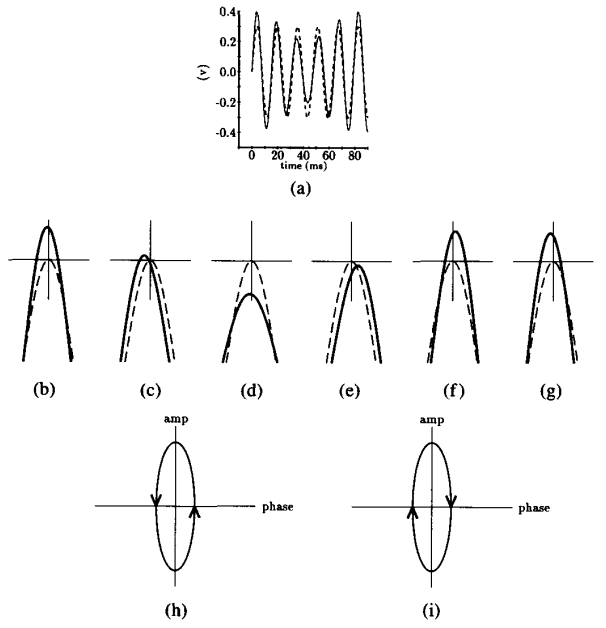

Fig. 1. Illustration of jamming avoidance computation. (a) Reference sine wave at 400 Hz (dashed) and beat pattern (solid) of 400- and 475-Hz signals. (b)–(g) Progress of the peak of the beat frequency around the reference for the six peaks of (a). This progression traces out an ellipse in the amplitude–phase state space, the direction of which is dependent on whether the reference is the lower (h) or the higher (i) of the two frequencies comprising the beat.

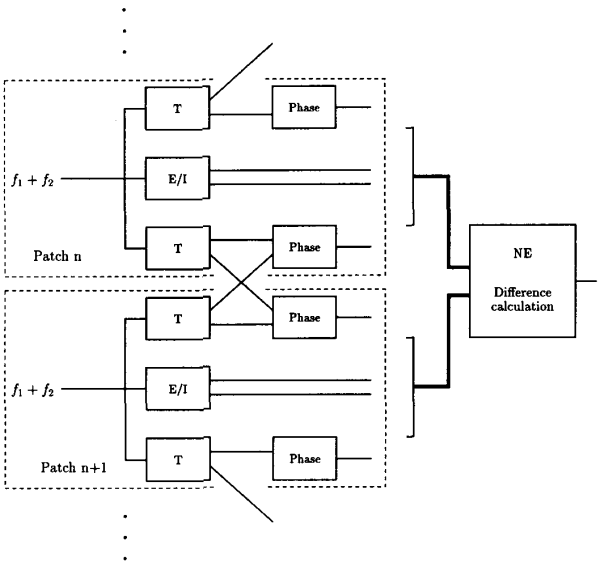

Fig. 2. Block-level diagram of JAR model.

the loop is traced as time progresses depends on whether the source frequency is higher or lower than the interference frequency. Let us define the difference frequency *Df* to be

$$DF = f_2 - f_1. \tag{1}$$

Df will be negative for a clockwise sense of rotation, and positive for counterclockwise rotations. Thus, the direction of rotation is a unique cue for the sign of the difference frequency.

The fish has no frequency reference, so the fish compares body patches with different amounts of interference to code correctly for the sign of the difference frequency. We now examine amplitude versus phase between body patches. The phase information is differential, and two adjacent body patches report opposite signs of rotation. The fish uses the patch with the larger change in amplitude to choose the correct orientation. Many computational elements come together to "vote"; each neuron's decision is weighted by the activity in the amplitude domain. The aggregate structure always codes correctly for the sign of the difference frequency, and thus the fish is able to adjust its source frequency away from the interference.

Weakly electric fish are expert at making accurate computations in the time domain from imprecise elements. Behaviorally, they can sense time differences down to 400 ns even though the jitter associated with a single sensory unit is in the 30-μs range [4]. They improve the time pathway jitter by converging many sensors to a few computational units. Thus, a hierarchical system is essential to their accuracy, and we incorporate this feature in our model.

III. Model Architecture

A block-level diagram of the JAR model is shown in Fig. 2. Each circuit, which computes the processing for one body patch, consists of an amplitude pathway and a phase pathway. Each body patch receives a signal comprised of two sinusoids of frequencies f_1 and f_2. These signals are added off chip. Different resistor ratios are used in the analog adders to represent different amounts of interference in each patch. The mixed signal is sensed by E/I-cells, which are sensitive to increases and decreases in peak-to-peak amplitude, respectively. The signal is also sent to the T-cells, which spike once per zero crossing of the signal.

At the next stage of the processing, each body patch computes a measure of differential phase using the outputs of the T-cells. Two pulse trains whose frequencies change over time are input to the circuit: The first comes from what we call the *reference* body patch T-cell, and the second comes from the *comparison* body patch T-cell. The circuit measures the delay between a pulse from the *reference* and the *comparison*. If the delay is decreasing, the circuit sends out a burst of voltage spikes. This burst represents a positive phase difference between the two input signals.

The amplitude and phase pathways finally come together in the NE circuit that models a structure at the top of the neural hierarchy of the fish. Each element identifies the sign of the difference frequency based on information

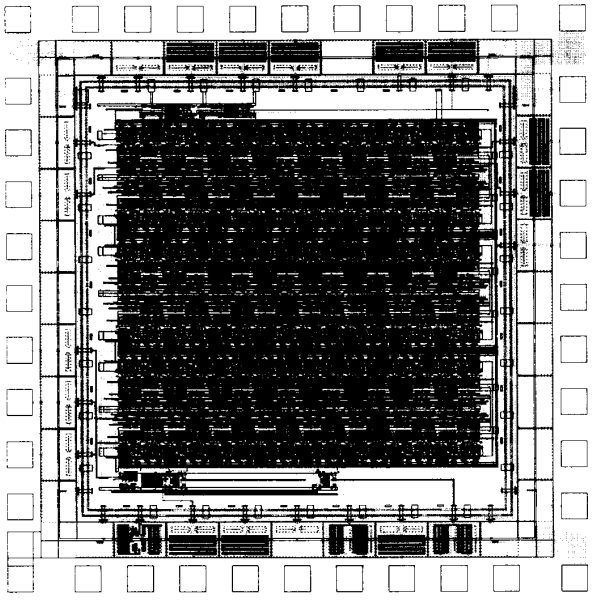

Fig. 3. Layout of 16-body-patch JAR system.

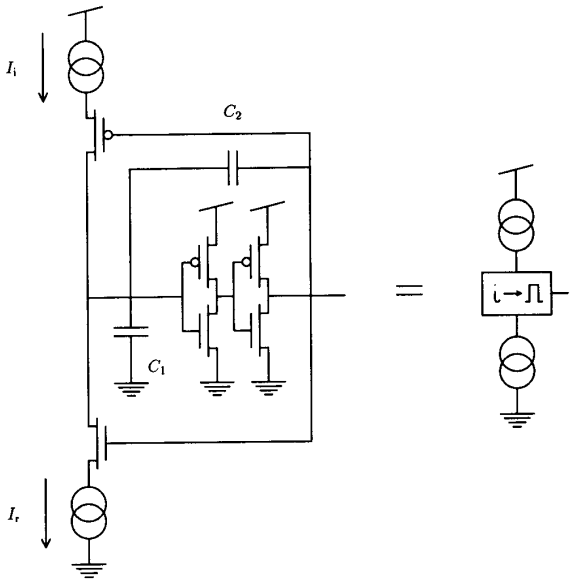

Fig. 4. Neuron circuit to convert an injected current to a spike train

obtained from one body patch alone. All the elements are combined in a nonlinear inhibition circuit weighted by the activity on the amplitude lines to determine the correct sign of the overall *Df*.

IV. Circuit Details

To test the model, we fabricated a 16-patch system on a 2.22-mm × 2.25-mm p-well chip (Fig. 3). All transistors are operating in the subthreshold regime with bulk grounded and well tied to V_{dd} unless otherwise specified.

All the levels in the circuit hierarchy communicate through frequency-modulated "nerve pulse" trains. Therefore, a basic component of each stage is a module to convert an injected current into a series of voltage spikes. This neuron circuit (Fig. 4), which is a slight variation of the ganglion circuit presented in [6], generates a series of short pulses, the frequency and duty cycle of which are

$$f = \left(\frac{1}{C_2 V_{dd}}\right)\left(\frac{I_i I_r}{I_i + I_r}\right) \tag{2}$$

$$\text{duty cycle} = \frac{I_i}{I_i + I_r}. \tag{3}$$

Both the amplitude and time pathways are only responsive to changes, so a sensitive derivative circuit was required (see Fig. 5). The input is passed through an amplifier with open-loop gain A to a nonlinear element [6] which feeds back to the amplifier. The nonlinear element has an input/output relationship that is approximately

$$I_{cap} = I_0 \sinh (V_{out} - V_{cap}). \tag{4}$$

For very small changes in input voltages, almost no current flows and the voltage on capacitor C_{hys} remains constant. The output is then just an amplified version of the input. For larger changes, the nonlinear element passes a current that is exponential in V_{out}, causing the voltage on the capacitor to rapidly equilibrate to the input voltage. Therefore, changes in the sign of the derivative (such as at the peaks of sine waves) create large voltage changes on the ouput.

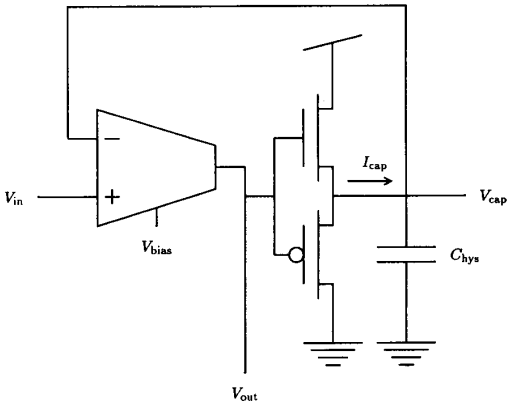

Fig. 5. Hysteretic differentiator circuit.

To obtain information about changes in peak-to-peak amplitude, we have designed the E/I-cell circuit shown in Fig. 6 that models the behavior of two types of cells in weakly electric fish [10]. Transistor Q_1 and capacitor C_1 form a filter that captures the envelope of the waveform presented at the input as long as the carrier frequency is significantly faster than any changes in amplitude. Leakage current I_l sets the rate of decay and determines the speed of response for the filter.

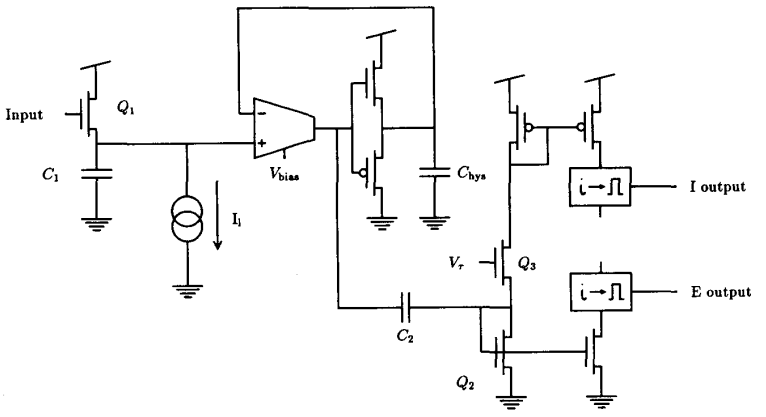

Fig. 6. Circuit implementation of E/I-cell.

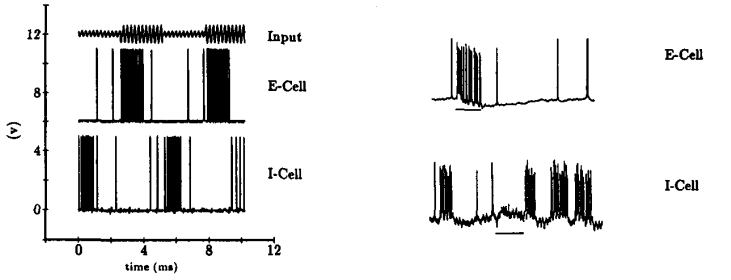

Fig. 7. (a) Circuit response of E/I-cell. Notice the transient response as circuit adapts. (b) Biological data on E- and I-cell. Bar shows time when step increase in amplitude was applied [10].

The output of the filter is then fed into the differentiator circuit described above. We take advantage of the properties of the differentiator to amplify the ripple during increases in the input envelope. During the smooth decay of the input filter, there is little change in the derivative, so there is very little change in the output. The output of the derivative circuit is ac coupled through capacitor C_2 to transistor Q_2. A rapid increase in voltage results in a current increase through Q_2, which generates voltage spikes on the E output. The current gradually decreases as the charge stored on C_2 is dissipated at a time constant set by the transconductance of Q_3. A similar sequence of events causes the I output to spike when a rapid decrease in voltage is coupled through C_2. The response of this circuit to a step increase and decrease in amplitude is shown in Fig. 7 along with data from an actual cell for a qualitative comparison.

The T-cell model (Fig. 8) uses two fixed-height, fixed-width pulse generators to create a spike at the zero crossing of each input waveform. The signal is first amplified against a voltage (V_{ref}), which we call the *zero level*. The large change in voltage is coupled into a rectification circuit, and is converted into a current pulse. The V_τ voltage on the coupling circuit sets the time course of the current spike and the dc level of current through the coupling cell. Capacitor C_1 of the neuron circuit takes this current impulse and causes the buffer formed by two CMOS inverters to change state. The second neuron is started by the first, with time delay set by the current through pass gate Q_1. Once the second neuron is on, it shuts off the first neuron. Thus, the pass gate sets the pulse width of the spike. Also, the second buffer ensures that there will be only one output spike per input current pulse.

In the next stage of processing, the model must make a comparison of these time markers from the T-cells. In the phase circuit (Fig. 9), a pulse coming in at In_1 charges capacitor C_1 to V_{dd}. The charge slowly leaks off through the leak transistor Q_1. When the next pulse comes in at In_2, the charge is shared between C_1 and C_2. This cycle repeats. If In_2 happens closer to In_1 than it did in the last cycle, there will be more charge on C_1 than on C_2, and the voltage on C_2 will increase. If In_2 happens later, C_2 will have greater charge than C_1, and the voltage on C_2 will drop. This change in voltage is ac coupled into a current rectifier that drives a neuron circuit (Fig. 10). Thus, the neuron will fire only for positive phase differences between the two inputs. There is evidence [4], [9] that the small cells in the fish perform this differential phase calculation, and the circuit analog is a good approximation to the functionality of the small cells (Fig. 11). In the

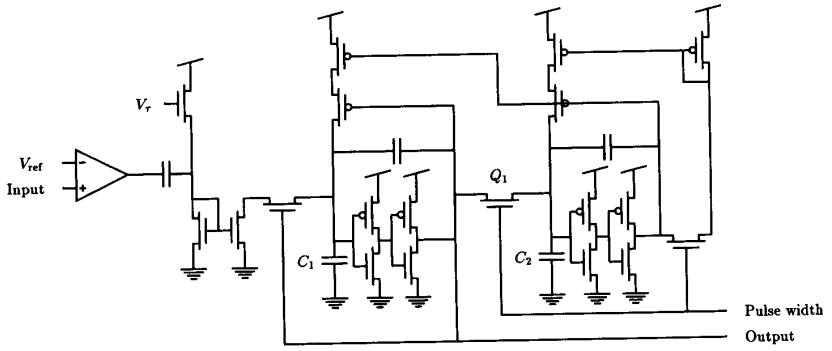

Fig. 8. Circuit implementation of T-cell.

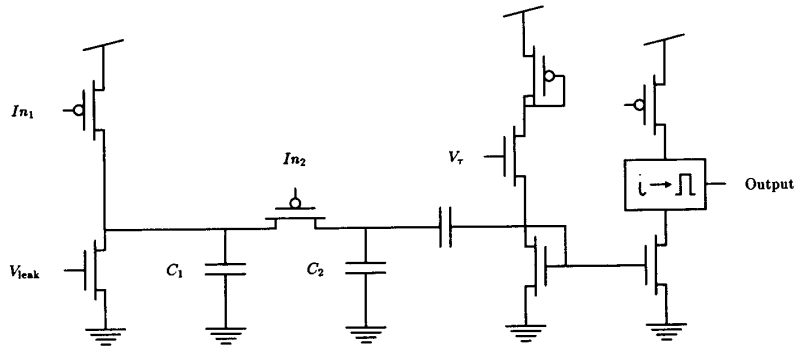

Fig. 9. Circuit implementation of phase circuit.

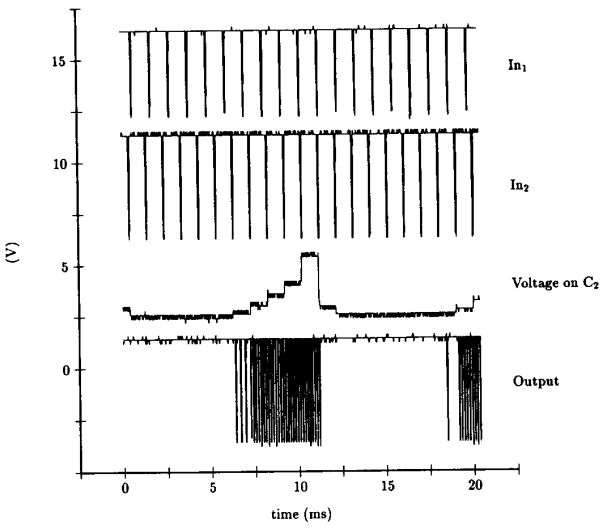

Fig. 10. Response of circuit to two pulse trains of different frequency. Notice activity of output when differential phase is between 0 and $\pi/4$.

biological system, there is an intermediate cell between the T-cells and the small cells which takes the output of many T-cells and improves the timing accuracy by averaging all of its inputs [4]. We have replicated that feature here by having many T-cells provide inputs to the phase circuit.

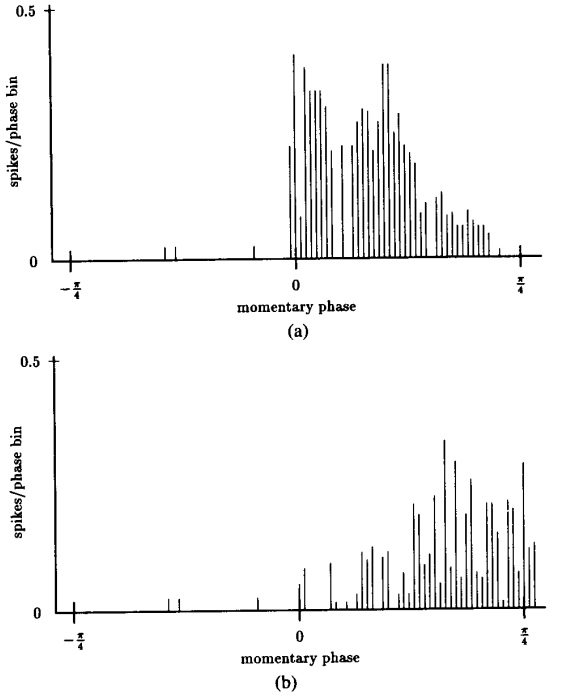

Fig. 11. Comparison of response of phase circuit to biological small cells computing differential phase in torus of *Eigenmannia*. (a) Response of phase circuit. (b) Response of biological small cells adapted from [5]. The ordinate shows mean number of spikes per phase bin, the width of each bin being equivalent to approximately 1°.

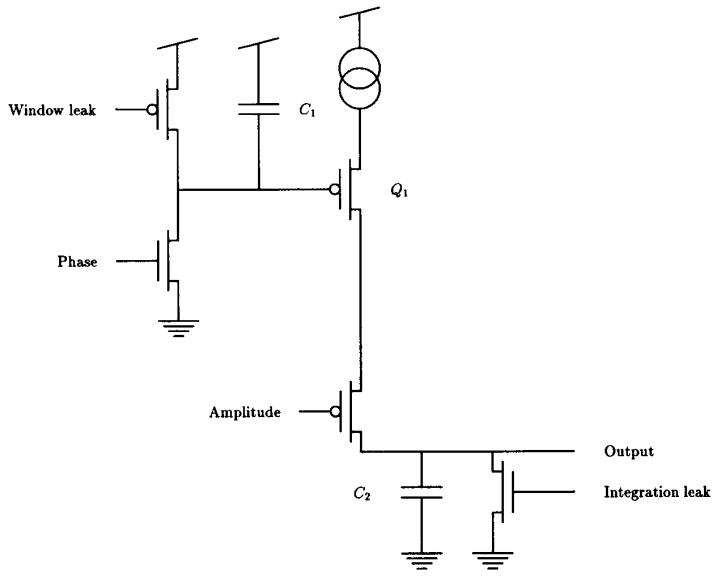

Fig. 12. Combination circuit to integrate amplitude and phase information.

To combine the amplitude and phase information, we must generate a signal that not only is dependent on the coincidence of the inputs, but also is proportional to the activity of the amplitude input. This task is accomplished by the combination circuit in Fig. 12. Spikes from the phase pathway are integrated on capacitor C_1 and open a window of activity by turning on transistor Q_1. The amount of time the window is open is set by the voltage on the window leak line. However, current can flow only when there is a spike on the amplitude input line. This current is integrated on capacitor C_2, making the output voltage proportional to the activity on the amplitude line, but only if the phase line is also active. The computation is done locally: phase and amplitude information come from the same body patch. There is a laminar structure in the fish that accomplishes the same task. One layer computes phase information, while the another receives inputs from the amplitude pathway. Phase and amplitude cell outputs that come from the same body area are aligned vertically in the fish [11] to make local computations easier to wire up.

In the final stage of the processing, we take the voltages coming in from the combination cells and choose the correct encoding for positive or negative difference frequencies. This stage mimics the behavior of the cells at the top level of processing in the fish, which are thought to be responsible for controlling a change in frequency of the electric organ discharge [13]–[15]. Table I outlines the four possibilities for the direction of the loop in the amplitude–phase space.

The final decision for the global sign of the difference frequency is made by the NE circuit in Fig. 13. The outputs from combination cells that code for a clockwise sense of rotation are connected to the V_{left} inputs, and the outputs that code for a counterclockwise rotation are connected to the V_{right} inputs. The NE circuit then performs a nonlinear inhibition, which is just the N-input generalization of the differential pair. If we bias the circuit with a subthreshold current I_b, the computation performed is

$$I_{\text{left}} = \mathrm{I}_b \frac{\sum_{\text{left}} e^{V_{\text{left}}}}{\sum_{\text{left}} e^{V_{\text{left}}} + \sum_{\text{right}} e^{V_{\text{right}}}} \tag{5}$$

$$I_{\text{right}} = I_b \frac{\sum_{\text{right}} e^{V_{\text{right}}}}{\sum_{\text{left}} e^{V_{\text{left}}} + \sum_{\text{right}} e^{V_{\text{right}}}}. \tag{6}$$

where all the voltages are scaled by kT/q. Thus, if any voltage on the left is a few kT/q larger than each of the voltages on the right, most of the bias current will be directed down the left side of the circuit. These currents are mirrored, and used to drive two final neuron circuits. If the difference frequency is negative, the left neuron fires; if the difference frequency is positive, the right neuron fires.

TABLE I
Df VALUES FOR DIFFERENT COMBINATIONS OF AMPLITUDE AND PHASE INFORMATION

Amplitude	Phase	Orientation	Difference Frequency
Increase	positive	CCW	positive
Increase	negative	CW	negative
Decrease	positive	CW	negative
Decrease	negative	CCW	positive

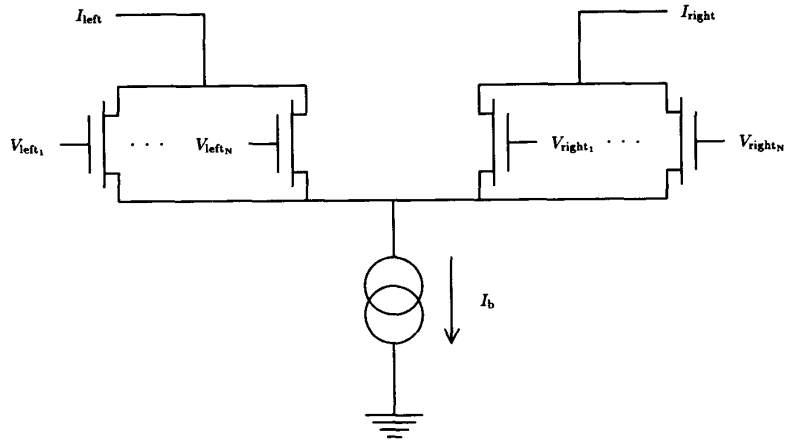

Fig. 13. NE circuit to do nonlinear inhibition.

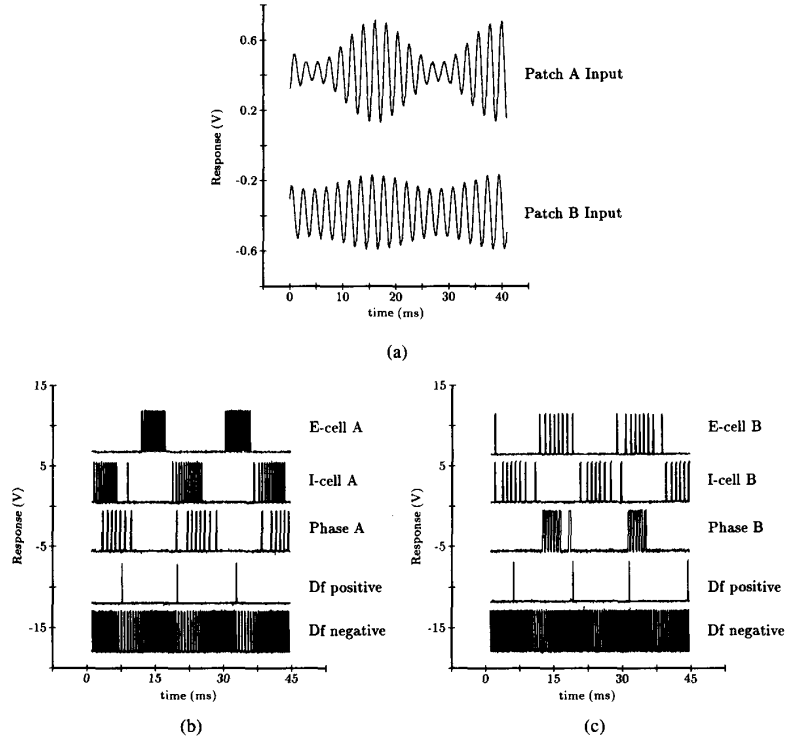

Fig. 14. Inputs and outputs from circuitry of two body patches. f_1 = 420 Hz; f_2 = 400 Hz. (a) Inputs to body patches A and B. (b) Patch A has more interference and stronger signal on E- and I-cell lines. Notice that I-cell and phase advance are in register indicating clockwise orientation. (c) Patch B has less interference, and erroneous counterclockwise information is ignored.

V. Results

We presented the system with two sine waves to simulate the electric organ discharges (EOD's) from two fish. Since we have encoded each stage of the hierarchy in pulse trains, we can make a direct comparison to the biological data. We will discuss the results obtained from two representative patches, referred to as patch A and patch B. We adjusted the mixing in body patches A and B such that there was less interference in B (Fig. 14(a)). The reference EOD (f_1) was presented at 420 Hz and the interference (f_2) was at 400 Hz. We see in Fig. 14(b) that the phase detector in patch A correctly fired when there was a decrease in EOD amplitude in body patch A. These signals correspond to a clockwise orientation in our amplitude–phase state space, and therefore to a negative differ-

ence frequency. In patch B (Fig. 14(c)), where there was less signal on the E- and I-cell lines, the phase circuit was firing with an increase in EOD activity, corresponding to a positive *Df*. Both patch A and B information converged on the combination cells and the NE nonlinear inhibition circuit. Since the information coming from patch A and B was weighted according to strength of the amplitude signal, the erroneous computation by patch B was discarded, and the correct global sign of the difference frequency was decoded (see Fig. 14).

VI. Discussion

An important problem in subthreshold CMOS circuits is the mismatch between devices. The biological model of jamming avoidance allows us to overcome this difficulty. The redundant information being sent up from the sensors to the computational elements averages out random fluctuations in the devices. No single element is accurate enough to code the timing information correctly. However, when used as an ensemble, the elements can resolve time differences with sufficient accuracy for the system to operate.

While the JAR computation requires higher time accuracy in the phase pathway, the most critical time constants were found in the E- and I-cells. Since the phase detection is a distributed computation, each phase cell can individually be less precise. However, each E- and I-cell computes information that pertains to one patch only. Their computation is done before the aggregation, thus they each need to be more accurate. This result is not immediately obvious from the architecture.

We have shown that local organization of sensory information is essential for correct jamming avoidance. Maintaining locality is a possible explanation for the spatial organization of the sensory information in the biological system. If the computation is performed over too large an area, or the comparisons are not made between adjacent body patches, an incorrect decision is made. If only local connections need to be made, and we assume we are optimizing wiring length, computational elements whose sensors are adjacent should also be adjacent. Thus, the model has shown a possible cause for a neural map of the fish's body surface.

We can see how defects in the system affect the performance by selectively disabling pieces of the model. Information critical to the decoding of the difference frequency can then be determined. Since there is a large amount of redundancy in the input sensors, no single phase or amplitude coder is critical to the processing. Furthermore, because of the inhibition circuit, even an erroneous signal will be corrected for by the weight of the other responses. Therefore, the large convergence from input to output makes the system robust.

The significance of modeling this biological system does not rest solely in the solution of the jamming avoidance problem. We can test aspects of the model that are technically difficult for the biologist to do with the behaving animal. Since the model was implemented on an analog VLSI chip, it runs in real time, and a wide variety of test conditions have been presented to the system without lengthy computer simulations. We can also close the feedback loop and let the chips control the frequency of the input sine waves. Then, multiple chips can interact to form a system of collective computational elements. The dynamics of such a system are not well understood, and a real-time model will be beneficial to such a study.

VII. Summary and Conclusions

We have designed and fabricated an analog VLSI model of the jamming avoidance response in electric fish. Modeling the electric fish has given us a novel approach for using distributed processing to calculate a global result which is robust to element failure. This processing is ideally suited for VLSI techniques due to its redundant nature. The VLSI model made an excellent approximation to the biological data obtained from behaving fish. Based on the success of the model, a larger chip with multiple patches and on-chip oscillators will be constructed to make a complete sensory-motor feedback system.

In the future, we will take the knowledge gained from our experience with the jamming avoidance response model and apply it to solving the problem of object detection and recognition using an array of sensors and a time varying electric field. This new system will make use of the high redundancy and the separation of the amplitude and phase pathways just as the JAR model did, however the computation performed will be of more general use in a signal processing environment.

Acknowledgment

The author would like to thank C. Mead for his invaluable assistance with this work. The model is based on many years of work by W. Heiligenberg, who first introduced me to electric fish. He and C. Shumway took part in several discussions of the model. Thanks also go to J. Lazzaro, M. A. Maher, J. Morrissette, and S. DeWeerth for reading and commenting on the manuscript.

References

[1] W. Heiligenberg, "Jamming avoidance responses," in *Electroreception*, T. H. Bullock and W. Heiligenberg, Eds. New York: Wiley, 1986, pp. 613–649.

[2] J. Bastian, "Electrolocation I: An analysis of the effects of moving objects and other electrical stimuli on the electroreceptor activity of *apteronotus albifrons*," *J. Comput. Phys.*, vol. 144, pp. 465–479.

[3] J. Bastian, "Electrolocation," in *Electroreception*, T. H. Bullock and W. Heiligenberg, Eds. New York: Wiley, 1986, pp. 577–612.

[4] C. E. Carr, W. Heiligenberg, and G. J. Rose, "A time comparison circuit in the electric fish midbrain. I. Behavior and physiology," *J. Neurosci.*, vol. 6, pp. 107–119, 1986.

[5] W. Heiligenberg and G. J. Rose, "Phase and amplitude computations in the midbrain of an electric fish: Intracellular studies of neurons participating in the jamming avoidance response of *eigenmannia*," *J. Neurosci.*, vol. 5, pp. 515–531, Feb. 1985.

[6] C. A. Mead, *Analog VLSI and Neural Systems*. Reading, MA: Addison-Wesley, 1989.

[7] J. P. Lazzaro and C. Mead, "Circuit models of sensory transduction in the cochlea," in *Analog VLSI Implementations of Neural Net-*

works, C. Mead and M. Ismail, Eds. Norwell, MA: Kluwer Academic, 1989, pp. 85–101.

[8] W. Heiligenberg and J. Dye, "Labelling of electroreceptive afferents in a gymnotid fish by intracellular injection of HRP; The mystery of multiple maps," *J. Comput. Phys.*, vol. 148, pp. 287–296, 1982.

[9] J. Bastian and W. Heiligenberg, "Phase sensitive midbrain neurons in *eigenmannia*; Neural correlates of the jamming avoidance response," *Science*, vol. 209, pp. 828–831, 1980.

[10] J. Saunders and J. Bastian, "The physiology and morphology of two types of electrosensory neurons in the weakly electric fish *apteronotus leptorhynchus*," *J. Comput. Phys. A*, vol. 154, pp. 199–209, 1984.

[11] C. E. Carr and L. Maler, "Electroreception in gymnotiform fish: Central anatomy and physiology," in *Electroreception*, T. H. Bullock and W. Heiligenberg, Eds. New York: Wiley, 1986, pp. 319–374.

[12] C. A. Shumway, "Multiple electrosensory maps in the medulla of weakly electric gymnotiform fish. I. Physiological differences," *J. Neurosci.*, vol. 9, pp. 4388–4399, 1989.

[13] J. Bastian and J. Yuthas, "The jamming avoidance response in *eigenmannia:* Properties of a diencephalic link between sensory processing and motor output," *J. Comput. Phys. A.*, vol. 154, pp. 895–908, 1984.

[14] G. Rose, M. Kawasaki, and W. Heiligenberg, "Recognition' units at the top of a neuronal hierarchy? Prepacemaker neurons in *eigenmannia* code the sign of frequency differences unambiguously," *J. Comput. Phys.*, vol. 162, pp. 759–772, 1988.

[15] M. Kawasaki and W. Heiligenberg, "Individual prepacemaker neurons can modulate the pacemaker cycle of the gymnotiform electric fish, *eigenmannia*," *J. Comput. Phys. A*, vol. 162, pp. 13–21, 1988.

John E. LeMoncheck received the B.S.E.E. degree from the University of California, San Diego, in 1988. He is currently a Ph.D. candidate in computation and neural systems at the California Institute of Technology, Pasadena.

During his undergraduate career he worked at NCR Corporation in the system architecture design group. He is now consulting for Synaptics Inc. designing neural network algorithms and VLSI architectures for pattern recognition.